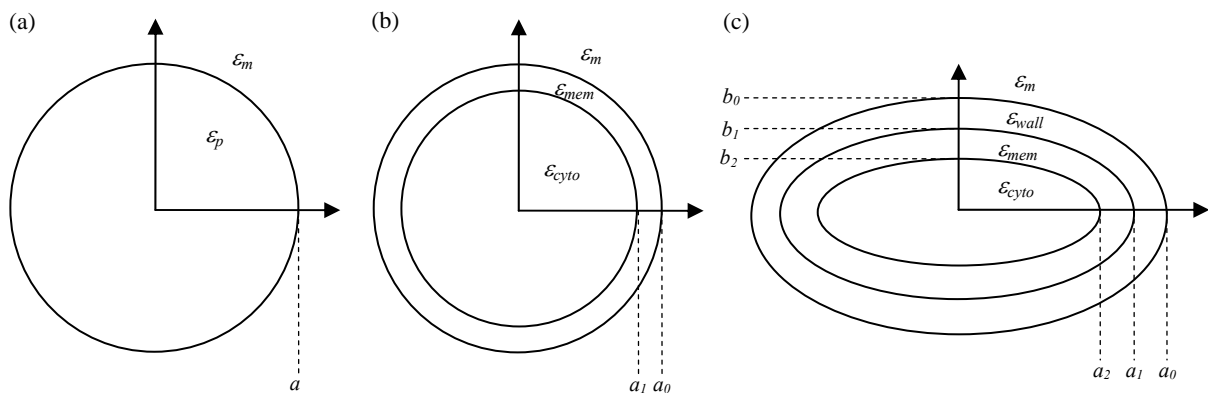


# Continuous dielectrophoretic bacterial separation and concentration from physiological media of high conductivity

Seungkyung Park,<sup>ab</sup> Yi Zhang,<sup>b</sup> Tza-Huei Wang<sup>\*bcd</sup> and Samuel Yang<sup>\*a</sup>

## S1. Modelling of dielectric responses of particles



**Figure S1.** Diagrams for electrical modelling of (a) homogeneous spherical (b) single shell spherical, and (c) double shell spheroid particles.

### Polystyrene beads

In the case of electric field with constant phase, time-averaged DEP force can be represented as,<sup>1</sup>

$$\langle F_{DEP} \rangle = \pi a^3 \epsilon_m \text{Re}\{K\} \nabla |E|^2 = 2\pi a^3 \epsilon_m \text{Re}\{K\} \nabla |E_{rms}|^2$$

where  $a$  is the particle radius,  $\epsilon_m$  is the permittivity of suspending medium,  $E$  is the electric field, subscript *rms* refers to a root mean square value, and  $K$  is the Clausius-Mossotti (CM) factor, which represents the effective polarizability of the particle with respect to the surrounding medium. For the polystyrene beads, homogeneous spherical particle model can be used (Figure S1a), and the CM factor is given by

$$K = \frac{\epsilon_p^* - \epsilon_m^*}{\epsilon_p^* + 2\epsilon_m^*} \tag{1}$$

where subscript  $p$  and  $m$  refer to the particle and the medium, respectively,  $\epsilon^*$  is the complex electric permittivity of the media, which can be represented as

$$\epsilon^* = \epsilon - j \frac{\sigma}{2\pi f} \tag{2}$$

where  $j = \sqrt{-1}$ ,  $\sigma$  is the conductivity,  $f$  is the electric field frequency. The conductivity of solid spherical particles can be represented as the sum of the bulk and surface conductivities, given by<sup>2</sup>

$$\sigma_p = \sigma_b + \frac{2K_s}{a} \tag{3}$$

where  $\sigma_b$  is the bulk conductivity, which is negligible for polystyrene beads,  $K_s$  is the surface conductance.

### Red blood cells

Red blood cells can be typically modeled as spherical particles with a concentric single shell, as shown in Figure S1b, representing cell cytoplasm surrounded by a membrane. The effective polarizability of this single shell particle can be represented with an equivalent homogeneous spherical particle with the modified particle permittivity incorporating the intrinsic effect of cell membrane, given by <sup>1</sup>

$$\varepsilon_p^* = \varepsilon_{mem}^* \frac{(a_0/a_1)^3 + 2 \left( \frac{\varepsilon_{cyto}^* - \varepsilon_{mem}^*}{\varepsilon_{cyto}^* + 2\varepsilon_{mem}^*} \right)}{(a_0/a_1)^3 - \left( \frac{\varepsilon_{cyto}^* - \varepsilon_{mem}^*}{\varepsilon_{cyto}^* + 2\varepsilon_{mem}^*} \right)} \quad (4)$$

where  $a_0$  and  $a_1$  is the outer radius of cytoplasm and membrane layer, respectively, subscripts *cyto* and *mem* refer to the cell cytoplasm and the cell membrane, respectively. By substituting the effective particle permittivity, the CM factor can be calculated.

### E. coli cells

*E. coli* cells generally have an elongated shape rather than a sphere, and require a more accurate dielectric modeling. We utilized a spheroid particle model with two outer shells, as shown in Figure S1c, representing cell cytoplasm surrounded by a cell membrane and a cell wall. The CM factor needs to be calculated based on the average value along each principal axes (*x*, *y*, *z*), which can be represented as <sup>3</sup>

$$K = \frac{1}{3} \sum_{k=x,y,z} K_k = \frac{1}{3} \sum_{k=x,y,z} \frac{1}{3} \left( \frac{\varepsilon_{1k}^* - \varepsilon_m^*}{\varepsilon_m^* + (\varepsilon_{1k}^* - \varepsilon_m^*)A_{0k}} \right) \quad (5)$$

where  $\varepsilon_{1k}^*$  and  $\varepsilon_{2k}^*$  are

$$\varepsilon_{1k}^* = \varepsilon_{wall}^* \frac{\varepsilon_{wall}^* + (\varepsilon_{2k}^* - \varepsilon_{wall}^*)A_{1k} + \lambda_1(\varepsilon_{2k}^* - \varepsilon_{wall}^*)(1 - A_{0k})}{\varepsilon_{wall}^* + (\varepsilon_{2k}^* - \varepsilon_{wall}^*)A_{1k} - \lambda_1(\varepsilon_{2k}^* - \varepsilon_{wall}^*)A_{0k}} \quad (6)$$

$$\varepsilon_{2k}^* = \varepsilon_{mem}^* \frac{\varepsilon_{mem}^* + (\varepsilon_{cyto}^* - \varepsilon_{mem}^*)A_{2k} + \lambda_2(\varepsilon_{cyto}^* - \varepsilon_{mem}^*)(1 - A_{1k})}{\varepsilon_{mem}^* + (\varepsilon_{cyto}^* - \varepsilon_{mem}^*)A_{2k} - \lambda_2(\varepsilon_{cyto}^* - \varepsilon_{mem}^*)A_{1k}} \quad (7)$$

and

$$\lambda_1 = \frac{a_1 b_1 c_1}{a_0 b_0 c_0}, \lambda_2 = \frac{a_2 b_2 c_2}{a_1 b_1 c_1} \quad (8)$$

$A_{ik}$  ( $i=1, 2, 3$ ) is the depolarization factor along each principal axes. For a prolate spheroid, it can be assumed that  $a_0 > b_0 = c_0$ , and this factor can be calculated as

$$A_{ix} = \frac{q_i}{(q_i^2 - 1)^{3/2}} \ln \{ q_i + (q_i^2 - 1)^{1/2} \} - \frac{1}{q_i^2 - 1} \quad (9)$$

$$A_{iy} = A_{iz} = \frac{1}{2}(1 - A_{ix}) \quad (10)$$

where  $q_i = a_i/b_i$ .

### CM factor calculation

In order to predict the DEP responses of particles and cells in this study, CM factor variation of each particle is calculated based on the theoretical models. The dielectric parameters used for the calculation are summarized in the Table S1. Figure S2 shows the

variation of  $\text{Re}\{K\}$  of the 1  $\mu\text{m}$  and 10  $\mu\text{m}$  polystyrene particles in DI water and TAE buffer, and *E. coli* and red blood cells in CSF and blood as a function of the electric field frequency.

**Table S1.** Parameters for the electrical modeling and CM factor calculation

Polystyrene beads <sup>2</sup>			
$\epsilon_p=2.55$ , $\sigma_b=0$ , $K_s=1.2\text{ nS}$ , $2a=1\text{ }\mu\text{m}$ and $10\text{ }\mu\text{m}$			
Red blood cells <sup>4</sup>			
	Conductivity (S/m)	Relative permittivity	Size ( $\mu\text{m}$ )
Cell cytoplasm	$\sigma_{cyto} = 0.31$	$\epsilon_{cyto} = 59$	$a_1 = 2.5$
Cell membrane	$\sigma_{mem} = 1 \times 10^{-6}$	$\epsilon_{mem} = 4.44$	$a_0 = 2.509$
<i>E. coli</i> cells <sup>3</sup>			
	Conductivity (S/m)	Relative permittivity	Size ( $\mu\text{m}$ )
Cell cytoplasm	$\sigma_{cyto} = 0.19$	$\epsilon_{cyto} = 61$	$2a_2 = 2.74$ $2b_2 = 2c_2 = 0.63$
Cell membrane	$\sigma_{mem} = 5 \times 10^{-8}$	$\epsilon_{mem} = 10.8$	$2a_1 = 2.75$ $2b_0 = 2c_0 = 0.64$
Cell wall	$\sigma_{wall} = 0.68$	$\epsilon_{wall} = 60$	$2a_0 = 2.79$ $2b_0 = 2c_0 = 0.68$
Suspending medium			
$\epsilon_m=78.5$ , $\sigma_m=0.0001\text{ S/m}$ (DI water), $0.12\text{ S/m}$ (8 mM KCl), $1.59\text{ S/m}$ (10X TAE), $1.8\text{ S/m}$ (CSF and blood)			

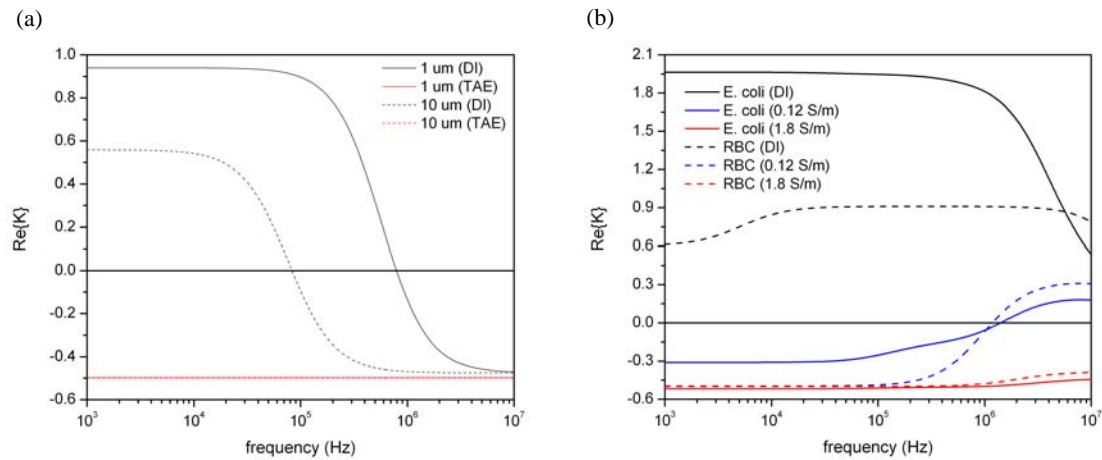


**Figure S2.** Real part of the CM factor for (a) 1  $\mu\text{m}$  and 10  $\mu\text{m}$  polystyrene particles and (b) *E. coli* and red blood cells at various medium conductivities.

## S2. Numerical simulation of particle trajectories

By assuming pseudo-equilibrium particle motion and the force equilibrium between Stokes' drag, DEP force, gravity, and particle lift force<sup>5</sup>, passive particle trajectories are calculated using COMSOL v3.5. Trajectories of 10  $\mu\text{m}$  and 1  $\mu\text{m}$  particles initially located at  $z=6\text{ }\mu\text{m}$  and different  $y$  positions are summarized in Figure S3. The mean inflow velocity is given as 0.01 m/s, corresponding to the experimental flow rate, with a parabolic profile in  $z$ -direction, and  $Re\{K\}$  is -0.5. Figure S3b and S3c show lateral displacements relative to the initial position at different lateral locations. Figure S3d and S3e show the variation in levitation height of each particle across the periodic domain length  $L$  at different lateral locations.

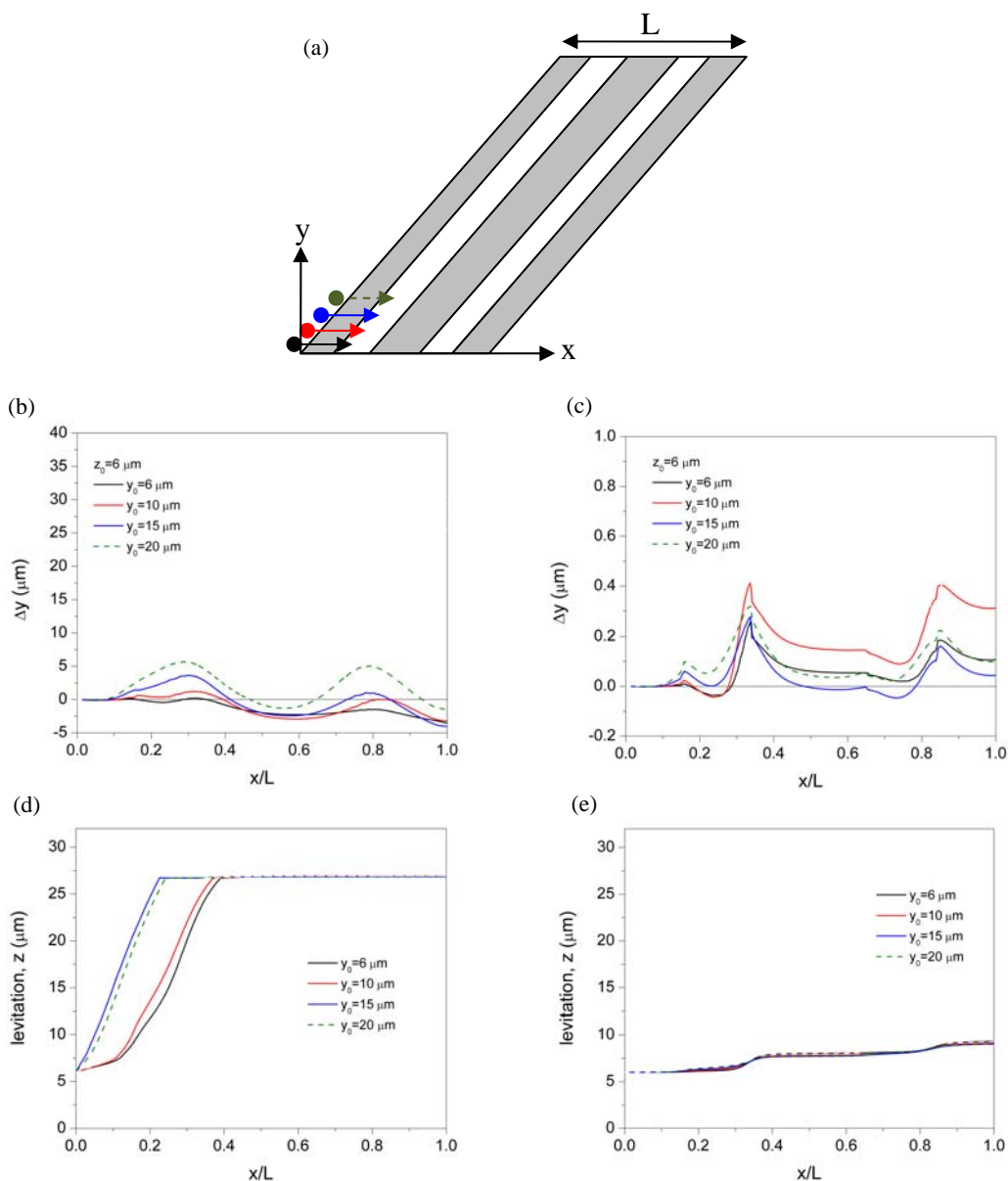


**Figure S3.** (a) illustration of initial particle positions. The change in  $y$ -directional particle displacement ( $y-y_0$ ) for (b) 10  $\mu\text{m}$  and (c) 1  $\mu\text{m}$  particles, and particle levitation height for (d) 10  $\mu\text{m}$  and (e) 1  $\mu\text{m}$  particles.

### S3. Device fabrication

The designed electrodes were fabricated on microscope slides using conventional photolithographic techniques. First, the microscope slide was cleaned with acetone and isopropanol. The slide was then rinsed with DI water and desiccated on a hot plate at 120 °C for 10 minutes. Positive photoresist (SC 1813, MicroChem) was spin-coated on the slide at 4000 rpm for 40 seconds. Soft baking was applied on a hot plate with ramped temperature variations, which were at 70 °C, 120 °C, and 70 °C for 2 minutes each. The photoresist layer was exposed to ultraviolet (UV) light for 100 mJ/cm<sup>2</sup> and was left in air at room temperature for relaxation. The substrate was then developed for 1 min and it was placed in reactive ion etcher for 10 seconds to remove any residues. After patterning the photoresist layer, a 10 nm-thick chromium layer and a 40 nm-thick gold layer were subsequently deposited on the substrate using e-beam evaporation chamber. By applying lift-off process in acetone, electrodes were obtained on microscope slide. Next, the PDMS channel was fabricated using a negative photoresist (SU-8 3025, MicroChem). The SU-8 photoresist was first spin-coated on a pre-cleaned silicon wafer at 2000 rpm for 1 minute, and soft baked on a hot plate at 65 °C and 95 °C for 20 minutes each. The photoresist film was then exposed to UV light for 200 mJ/cm<sup>2</sup> and post baked on a hot plate at 65 °C and 95 °C for 20 minutes each. The exposed layer was developed for 15 minutes and hard baked at 200 °C for 2 hours. The height of the developed channel mold was measured as 32 µm using a profilometer. Subsequently, the PDMS mixture (Sylgard 184, Dow Corning) in 10:1 ratio of prepolymer and curing agent were prepared. After degassing in a vacuum chamber, the PDMS mixture was poured over the mold and cured at 70 °C for 1 hour. The PDMS layer was then peeled off from the master and access holes were punched using a syringe needle. Lastly, the PDMS channel and the electrode deposited slide were treated with oxygen plasma at 30W for 1 minute and bonded together to obtain an enclosed microfluidic channel. The final device is shown in Figure S4.

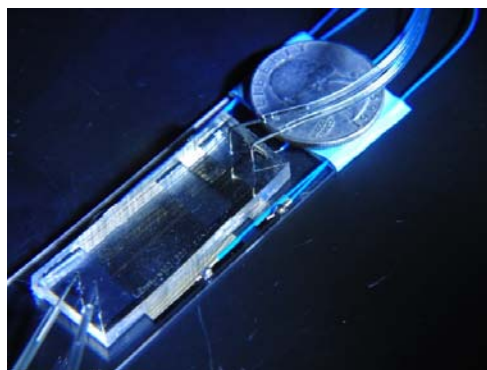


**Figure S4.** Photograph of the fabricated microfluidic device

### References

1. T. B. Jones, *Electromechanics of Particles*, Cambridge University Press, Cambridge, 1995.
2. T. Sun, D. Holmes, S. Gawad, N. G. Green and H. Morgan, *Lab Chip*, 2007, **7**, 1034-1040.
3. K. Asami, T. Hanai and N. Koizumi, *Biophys. J.*, 1980, **31**, 215-228.
4. A. Valero, T. Braschler and P. Renaud, *Lab Chip*, 2010, **10**, 2216-2225.
5. Y. Huang, X. B. Wang, F. F. Becker and P. R. Gascoyne, *Biophys. J.*, 1997, **73**, 1118-1129.